ChemComm

Check for updates

Lanthanide-based logic: a venture for the future of molecular computing

Sofia Zanella, [ID] Miguel A. Hernández-Rodríguez, [ID] Rute A. S. Ferreira [ID] and Carlos D. S. Brites [ID] *

Managing the continuous and fast-growing volume of information, the progress in the Internet-of-Things, and the evolution from digitalization to networking are huge technological chores. Si-based integrated chips face increasing demands as they strive to meet these challenges. However, there is growing recognition that information processing and computing based on molecules performing logic operations may play a decisive role in shaping the future of the computer industry. Molecular logic gates are molecular counterparts of electronic devices that, instead of exclusively by electrical signals, can be stimulated by diverse chemical or physical input signals that produce optical outputs according to a well-defined logical transfer function. Several materials have been applied for molecular logic, however, the Ln^{3+}-based ones appear to be a commendable choice, as they can respond to both chemical and physical stimuli, presenting unique photophysical properties that make them quite popular for photonics applications. Here we critically review illustrative molecular logic systems based on Ln^{3+} ions and discuss their potential for integration in future molecular photonic–electronic hybrid logic computing systems.

Introduction

There is endless demand for new and smaller computing devices. Information technology is one of the areas that has significantly improved the well-being of the common citizen in the last few decades. Since the first digital-programmable computer was developed, information technologies have been upgraded based on front-edge fabrication technology that integrates an increasing number of electronic components in a single chip.[1] In a few decades, computers and their related systems have become smaller due to the substantial scalable shrinkage of silicon-based technology components.[2–4] While silicon-based devices continue to play a central role in computing,[1] it is now accepted that bottom-up technology has the potential to enhance the current state-of-the-art (Fig. 1).[5] Quantum computing[6] is perhaps the most well-known example, but other alternatives include molecular computing[7] and photon manipulation.[8] Another alternative approach exploits molecules as the fundamental building blocks for information

Phantom-g, CICECO – Aveiro Institute of Materials, Department of Physics, University of Aveiro, 3810-193 Aveiro, Portugal. E-mail: carlos.brites@ua.pt

Sofia Zanella is a PhD student in the Physics Department of the University of Aveiro and CICECO – Aveiro Institute of Materials. Her doctoral studies are focused on the application of Ln^{3+}-containing materials for logical devices and temperature sensors based on the spectroscopic properties of Ln^{3+} ions.

Sofia Zanella
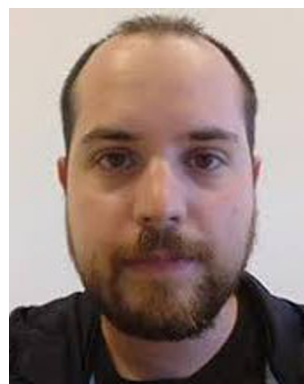
Miguel A. Hernández-Rodríguez is a researcher in the Physics Department of the University of Aveiro and CICECO – Aveiro Institute of Materials. His research interests focus on nano-materials doped with lanthanide ions under extreme conditions for sensor and photonics applications, and on molecular logics using trivalent lanthanide ions.
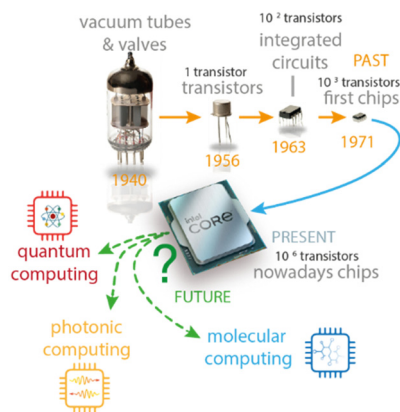
Miguel A. Hernández-Rodríguez

Fig. 1 Schematic timeline of computing systems since the vacuum tubes and valves to the present chips. Future computing strategies, still under development, include quantum, photonic or molecular computing.

processing, utilizing Boolean algebra concepts introduced by de Silva in 1993.[9] Although molecules capable of performing basic arithmetic operations, such as '1 + 1 = 2' may not seem like much competition for silicon circuitry,[10] they represent a significant step forward and have motivated the development of new molecules able to mimic electronic counterparts. Despite the evident potential of molecular logic, the current state of solution-based molecular devices, which respond to chemical stimuli and produce optical outputs, is mainly limited to proof-of-concept devices. This is true essentially for complex information processing because both the emission and absorption of radiation are, in general, isotropic, not readily allowing a single molecule to communicate specifically with another. Such shortcomings have motivated the research on new emitting centres able to combine narrow emission lines that can operate also in a solid-state when interrogated by chemical (*i.e.*, chemical

species) or physical (*i.e.*, electrical, magnetic, thermal stimulus) inputs. Among diverse emitting centres, trivalent lanthanide ions (Ln^{3+}) are one of the most promising candidates because there is historical background on their application to photonic devices due to their unique emitting features. In this work, after the principles of Boolean algebra and a historical perspective, we revise in detail some literature examples of molecular logic based on the emission of trivalent lanthanide ions. We will first discuss some molecular logic examples of a Ln^{3+} based system that operates exclusively in wet conditions. In the last section, we will report some illustrative examples of Ln^{3+} molecular logic through physical inputs, where some of them include the recent contributions from our group of molecular logic gates in the solid state. At the end of this review, we offer a perspective on the potential applications of molecular logic using Ln^{3+} ions and discuss the future opportunities for the development of Ln^{3+}-based logic as an innovative approach to the field of molecular computing.

Basics of Boolean logic

The concepts of Boolean algebra and logic operations

Binary or Boolean logic, proposed in 1847 by George Boole, is the core concept of Boolean algebra that forms gates which are the base for the construction of all digital electronic circuits and microprocessors. In computing, the term "Boolean" refers to a result that can only assume one of two possible values: "TRUE" or "FALSE". Boolean algebra may be implemented binary variables and logic operations in which all the possible values are 1 or 0. Through the use of logic elements, also known as inputs, combined in various combinations, Boolean operations generate a set of results, referred to as outputs, which are typically presented in a truth table (Fig. 2).[11] While initially applied in electronic circuits, the principles of Boolean logic

Rute A. S. Ferreira

Rute A. S. Ferreira is an Associate Professor in the Physics Department of the University of Aveiro and vice-director of CICECO-Aveiro Institute of Materials. Her research interests are the light emission of sol–gel derived organic/inorganic hybrids without metal activator centres and doped with lanthanide ions featuring applications in photonics (phosphors, solid-state lighting, and integrated optics) and photovoltaics (luminescent solar concentrators), the photophysical behaviour and optoelectronic properties of crystalline and amorphous nanoparticles of semiconductor and oxide materials functionalized with organic capping via wet chemical reactions and spectroscopic ellipsometry, including optimization of modelling algorithms.

Carlos D. S. Brites

Carlos DS Brites is an Assistant Professor in the Physics Department of the University of Aveiro. His research interests are focused on the application of trivalent lanthanide based molecular materials such as nanoparticles for molecular logics and computing using physical inputs. Besides that, he also has interest in the characterisation of Ln^{3+}-based thermometers as luminescent nanotools for probing nanoscale heat transport in solids and nanofluids.
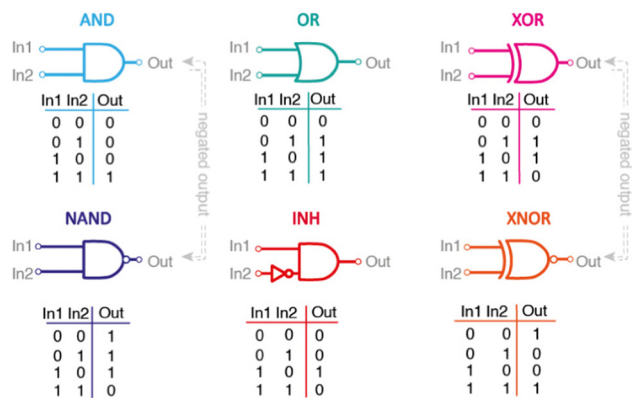
Fig. 2 Designation, representation, and truth table for the most common binary operations with two logic inputs (In1, In2). The truth tables list the correspondence between the combination of the inputs and the logic output (Out).

can be extended to diverse inputs and outputs irrespectively of their nature, such as those able to stimulate molecules, opening the field of molecular logic. Unlike conventional electronic devices that process electrical inputs and generate electrical outputs, molecular logic devices utilize chemical or physical stimuli, such as light, heat, electricity, or magnetism, to produce logic outputs, often resulting in changes in the physical properties of the material.[2]

The response of a logic system to a physical or chemical stimulus can be numerically translated into logic outputs of "1" or "0," respectively. In the positive logic convention, the presence of an input (logical input value of 1) may yield an output above a defined threshold, representing an ON output (logical value 1). Conversely, if the response output is below the defined threshold, the logic value is 0.

Simple logic operations, such as YES and NOT gates with a single input, exhibit specific responses where inputs of 0 and 1 produce logic outputs of 0 and 1, respectively. The 2 inputs-1 output logic operations allow more options. As an example, to describe an AND logic gate the only possibility to reach an output of logic value of 1 is to have both inputs as 1. By combining simple logic operations, more complex operations can be achieved, such as binary number subtractors and adders, or multiplexing and demultiplexing signals.[12] Sequential logic refers to a logic system that depends on the combination and sequence of inputs, with the KEYPAD LOCK being an example of a molecular logic implementation reported by Margulies *et al.* in 2007.[13] Another key concept, useful to understand some examples discussed hereafter is logic reconfiguration, wherein a single gate can perform different logic operations depending on the selected output.[14] This characteristic of logic reconfiguration is commonly associated with molecular logic and is relatively uncommon in conventional electronic devices.

Furthermore, in electronic logic gate circuitry, the typical convention between the "off" and "on" states is at least a factor of 2. This convention ensures that the voltage levels representing the "on" and "off" states are set well above the detection

limit of the system yielding a reliable detection, even in the presence of noise. In the case of a molecular logic device, this convention is not defined because the decision of a threshold between the states "on" and "off" depends on the specific output and on the noise level of the logic readout. Nevertheless, general guidelines for selecting an appropriate threshold should keep a spacing between points on the states "on" and "off" higher than 2 times the uncertainty on the determination of that state.

History from the first molecular logic to the current approaches

It is interesting to notice that molecules have been understood since the first steps of electronics as counterparts for electronic devices. In 1956 it was reported for the first time by Hirshberg, the possibility for molecules to have memory,[15] mentioning that such phenomenon is the first reversible photochemical process which has essentially the same features as the "high-speed memory", a term used for what was later known as random-access memory (RAM). Fig. 3 gives a timeline overview of the main milestones of molecular logic devices.

In 1974 Aviram wrote a fundamental work that grounded the field of molecular electronics, reporting the first molecules that mimic the properties of electronic devices.[16] Later, in the 1990s de Silva defined for the first time an AND logic operation that could respond to the presence of two different ions.[9] The first works reporting molecular logic based on Ln^{3+} ions date from 1998 and consisted in a NAND gate[17] followed by an INHIBIT gate in 2000.[18]

The first generation of molecular logic devices dates from the 2000s, and significant progress has been made in the design of molecular logic systems based on photochemical,[19,20] electrochemical,[21] and biochemical interactions.[22,23]

Afterward, it was recognized that molecular species can perform complex logic operations such as adding and subtracting binary numbers, multiplexing and demultiplexing a logical signal,[19,24] and also, sequential logic functions (*e.g.*, counters, latches, flip-flop, *etc.*).[4,25] As most of these logic devices required wet conditions to operate, their immediate prospective use was in biomedicine. Molecular and biomolecular computing/logic systems,[26] including supramolecules,[27] proteins,[28] DNA,[29,30]
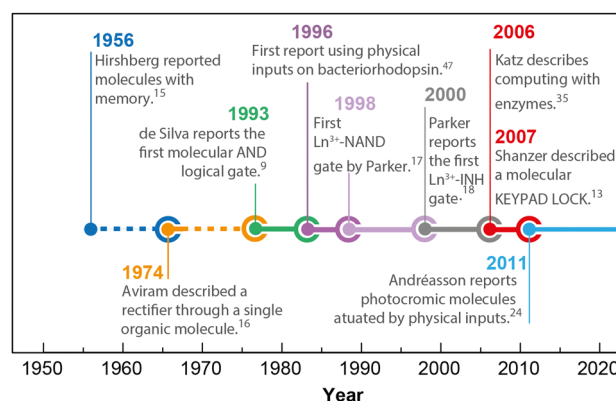

Fig. 3 Some milestones in molecular logic between 1956 and 2022.

DNA/conjugated polymer systems,[31] and enzyme-based systems,[32] have been used to process chemical and physical input signals mimicking most of the logic operations of semiconductor-based electronic devices, with promising advantages. One of the most claimed is parallel computing, as the signal processing is performed by molecules and parallel computation is accessible (if it is possible to address them) allowing a virtual exponential gain on the computing power in comparison with current electronic devices.[33] Although these results constituted a clear breakthrough, until now, none of these molecular devices were able to effectively replace a single electronic counterpart with gain in terms of computing performance.[34] Among the diverse limitations noticed, the concatenation of logic elements, a fundamental requirement for logic assembly, by which one logic gate feeds the next one in a controlled and traceable way, is probably the most difficult to overcome so far, and thus few reports of concatenation have been published involving molecular logic gates.[35–37]

Recent research in the field has involved molecular computation identification,[38] sensing,[39] gaming,[40] and cryptography.[41] Among these new challenging research studies, the ones that use biomolecules are also the ones with the highest level of computational power so far.[41] Inside live cells, for example, where semiconductor-based devices have some incompatibilities, molecular logical computation can be extremely useful. Furthermore, molecular and biomolecular steganographic systems in which a precise chemical stimulus leads to an appearance of a text message can be created by photonic crystals, fluorescent materials, bacteria, or antibodies. In a recent review by Liu et al. the diverse applications of logic gates in the last 5 years are summarized to discuss the research progress in the field.[42] Additionally, several comprehensive reviews on molecular logic have been written in the last decade.[43–46]

Physical inputs and photochromic molecules

Molecular logic devices involving only physical inputs are based on light-matter interactions. The first report from 1996 studied bacteriorhodopsin films,[47] but the field quickly evolved to the use of photochromic species capable of performing combinatorial logic gates (AND, XOR, INH) to binary and sequential operations (KEYPAD LOCK, HALF-ADDER, HALF-SUBSTRACTOR). The photochromic molecules are characterized by the switch from one isomer form to another in the presence of a light stimulus, the so-called photoswitching.[48,49] Usually, photochromic molecules respond to external stimulation such as light and generally, one isomer absorbs in the UV region. Some examples of such molecules are spiropyran and diarylethene. The design and synthesis of photochromic molecules have received more attention in the past few years, due to the possibility of exploiting these molecules to perform logic operations based on resonant energy transfer (FRET) or photoinduced electron transfer (PET).[50] The possibility to incorporate different photochromic components makes the resultant system suitable for absorption and emission at different wavelengths.[51]

In 2011 Andréasson et al. presented a pioneer work on molecular logic systems exploiting exclusively physical inputs.[24] Using UV radiation (input 1: 392 nm and input 2: 302 nm) the photoisomerization of the FG-DTE organic molecule was induced, changing the molecule from an open to a closed form. Recording different outputs as the absorbance at different wavelengths (535 and 393 nm), the emission at 312 nm and the shift of the absorbance is possible to describe AND, INHIBIT, XOR and INHIBIT gates, respectively. The system reported allows a further definition of complex operations as HALF-ADDER, HALF-SUBSTRACTOR, MULTIPLEXER, DEMULTIPLEXER, and KEYPAD LOCK. More examples on this topic were reported in a recent review by the same group and the reader is referred to ref. 52 for further details. Nevertheless, most photochromic molecules suffer from severe photobleaching, and low chemical stability over time, and the operation is often under wet conditions. Therefore, durable luminescent materials are required to develop a new class of molecular logic devices. Among the distinct emitting centres reported so far for molecular logic, Ln^{3+} containing materials (both inorganic crystals and β-diketone complexes) appear as good candidates as an alternative to photochromic molecules.

Lanthanides ions for molecular logic

Why are lanthanides ion so appealing in molecular logic?

At first sight, trivalent lanthanide ions (Ln^{3+}) seem not very attractive to molecular logics and sensing applications: the spherical entities with "inner" 4f valence electrons interact electrostatically with their surroundings, display little stereochemical preferences, and have very similar chemical behaviour.[53] However, these ions exhibit rich and unique spectroscopic and magnetic properties that can be applied using spectroscopic and magnetic stimuli or to construct materials with virtually on-demand photophysical and chemical properties. Moreover, since the ions adapt easily to almost any chemical environment and can therefore be readily introduced into a variety of ionic situations, the Ln^{3+} ions can act as functional centres in molecular and supramolecular edifices. For a seminal review paper on Ln^{3+} ions focused on unique spectroscopic and magnetic properties the reader is referred to ref. 53. Furthermore, in 1964 Melby reported a seminal work focusing on the synthesis of Ln^{3+} complexes.[54] For most applications, the trivalent lanthanides are usually combined with organic or inorganic ligands to improve their luminescence properties, and in the case of molecular logic, it is possible to exploit the energy transfer mechanism that occurs between the energy levels of ligands and those of Ln^{3+} ions.

In the literature most reported molecular logic gates are working with chemical inputs, such as the concentration of some ions, pH, or the presence of molecules that can stabilize the system. Nevertheless, external stimuli, such as light, temperature, magnetic, and electric fields could induce changes in the electronic transition of the material based on Ln^{3+}. These ions typically emit in a wide wavelength range covering the

UV-VIS-NIR spectral regions, with characteristic line-like emission bands (<10 nm) and long-lived excited state lifetimes (>10 µs).

It is established that trivalent Ln^{3+} ions can improve state-of-the-art molecular logic devices, despite only a handful of them having been reported so far.[55–57] Ln^{3+}-based emission is relevant for molecular logic because it is possible to translate the modifications of narrow-band emission spectra and characteristic colour changes observed by naked eyes to basic 0 and 1 states for logic binary systems. Furthermore, the possibility of having multiple outputs can generate different logic operations under the same input conditions, which could increase the information content in the logic library and further improve the information processing capability. Usually, systems based on lanthanides are widely used in lighting, displays, laser, security ink and marking, barcoding, multi-analyte detection, theragnostic, biomedical analyses, and imaging with the potential to follow metabolic pathways.[58–61] To date, most of the logic gates based on Ln^{3+} ions respond to chemical inputs and thus operate exclusively in wet conditions. Therefore, this review aims at reporting some illustrative examples of Ln^{3+}-based molecular logic gates, stressing future challenges of exploiting physical inputs.

Ln^{3+}-based molecular gates actuated by chemical inputs

One of the first logic gates based on Ln^{3+} was reported by Gunnlaugsson et al. in 2001,[62] a Tb^{3+} tetraazamacrocyclic complex sensitive to the presence of H^+ and molecular oxygen (O_2) was investigated as a molecular-logic device. The emission of the Tb^{3+} complex upon 330 nm excitation switches to the on state (logic output 1) only in the presence of H^+ and in the absence of O_2. Exploiting the emission intensity of Tb^{3+} as the logic output, the logic gate with a transfer function corresponding to a two-inputs (H^+ and O_2) INHIBIT (Fig. 4a) was described. L. Wang et al.,[63] in 2012, reported a luminescent probe based on an organic europium complex ($Eu(DBM)_3DPPZ$) that detects AcO^- and O_2 ions (DBM and DPPZ stand, respectively, for dibenzoyl methane and dipyrido[3,2-a:2′,3′-c]phenazine). The logic output was the emission intensity of the $^5D_0 \rightarrow {}^7F_2$ transition of Eu^{3+} at 610 nm. The authors studied the response of the complex to different gases such as air, N_2, and O_2. In this system, the emission intensity increases upon the addition of AcO^-, which is enhanced when AcO^- reaches about 4 equivalents of Eu^{3+}.

These authors rationalized their observations based on the substitution of DPPZ (which is weakly coordinated to the Eu^{3+} complex) by the AcO^- ion. The emission intensity increases upon the addition of AcO^-, but when the concentration of this ion reaches 4 equivalent the system reaches saturation. In the case of oxygen ions, the intensity of the Eu^{3+} transition ($^5D_0 \rightarrow {}^7F_2$) decreases with the increase of the concentration of O_2. The conversion of the results into a logic gate leads to defining an IMPLICATION gate, a two inputs logic operation where the output is 0 only when the two inputs are 1 and 0.

Another work exploiting O_2 as the logic input was reported by M. de Susa et al.[67] on the photophysical properties of a
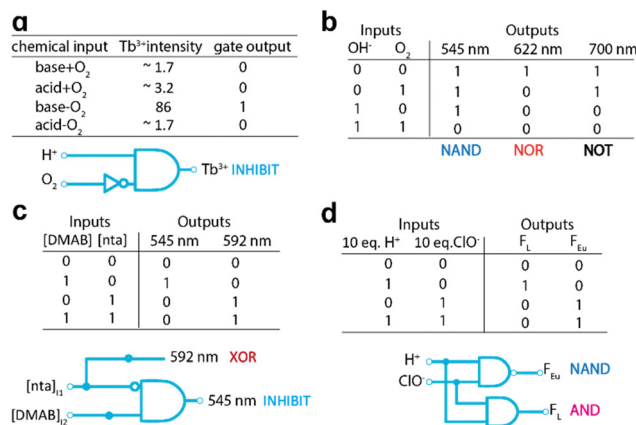

Fig. 4 (a) INHIBIT gate described by Gunnlaugsson et al. in 2001. Adapted with permission from ref. 62. Copyright 2001, American Chemical Society, licensed under a Creative Commons Attribution (CC by 3.0) License. (b) NAND, NOR, and NOT logic gates demonstrated by C. S. Bonnet. Adapted with permission from ref. 64. Copyright 2009, American Chemical Society (c) INHIBIT and XOR gates by Truman et al. Adapted with permission from ref. 65. Copyright 2013, Wiley-VCH Verlag GmbH & Co. KGaA, Weinheim. (d) AND and NAND gates by Z. Zhou et al. Adapted with permission from ref. 66. Copyright 2019 Elsevier Ltd.

Eu^{3+} complex combined with 1,8-naphthalimide ligand (L), at a stoichiometric ratio Eu/L of 1:1. A logic gate was defined using the presence or absence of oxygen (input 1) and the Eu^{3+} concentration above a threshold level defined as 2 times the Eu^{3+} concentration $>$ L (input 2). The emission of Eu^{3+} in the red spectral region (essentially the $^5D_0 \rightarrow {}^7F_2$ transition) is observed only if O_2 is excluded and the Eu^{3+} concentration surpasses the threshold value set. This led to a truth table characteristic of an INHIBIT logic function.

H. Chen et al.[68] reported a system based on the Eu^{3+} cyclen complex for multiple sensing of metal ions in an aqueous solution. The complex is composed of three main parts: (i) the terpyridine, sensitive to Eu^{3+}, and a receptor for transitions of other metal ions; (ii) the cyclen unit made the complex soluble in water; and (iii) the Eu^{3+} ion, playing the role of a central processing unit (CPU) and giving a photoluminescence output to the molecular robot. After testing different metal ions as the logic inputs, three logic gates were built. In the first logic gate (OR gate) the concentrations of H^+ and Fe^{2+} ions were exploited as the logic inputs (presence and absence of the ions taking respectively the logical value 1 and 0), and the logic output, was defined based on the absorbance at 325 nm. Changing the detected ion by Mn^{2+}, a YES gate was defined using the relaxivity of the Eu^{3+} complex as the logic output. Moreover, sharing the same logic inputs (the H^+ and Zn^{2+} ion concentration), it was possible to design INHIBIT and OR logic gates, analysing distinct readouts: the intensity of Eu^{3+} transition $^5D_0 \rightarrow {}^7F_2$ near 617 nm and the absorbance at 325 nm, respectively. In general, systems based on Eu^{3+} emission are very often used for ion sensing. L. Lu et al.[69] noticed that, using enoxacin (ENX) to sensitize the luminescence of Eu^{3+} the presence of Ag^+ and SCN^- ions can be applied for molecular logic, as only the simultaneous presence of both ions enhance

the emission intensity of the $^5D_0 \rightarrow {}^7F_2$ transition of Eu^{3+} (monitored at 614 nm) defining an AND gate.

In 2009 a joint work by T. Gunnlaugsson and C. S. Bonnet[64] reported a stoichiometric combination of an Eu^{3+} based complex of a quinoline derivatized cyclen and Tb^{3+}-based quinoline-cyclen. The changes in the emission intensity, observed in the solution prepared with both Ln^{3+} systems, are chosen as the logic output and the pH and concentration of O_2 are used as the logic inputs, defining distinct combinatorial logic gates. Therefore, by studying the emission intensity at 545 (Tb^{3+}, $^5D_4 \rightarrow {}^7F_5$), 622 ($Eu^{3+}$, $^5D_0 \rightarrow {}^7F_2$), and 700 nm ($Eu^{3+}$, $^5D_0 \rightarrow {}^7F_4$), the authors demonstrate that it is possible to define, respectively, NAND, NOR, and NOT logic gates (Fig. 4b). In this work[64] the logic outputs are defined analysing the emissions from both Eu^{3+} and Tb^{3+} ions, whereas in the former work of 2001,[62] the logic outputs were defined using only the emission of a single emitting centre (Tb^{3+}).

The same two emitting centres were studied in 2015 by Bradberry et al.,[70] who reported Eu^{3+} and Tb^{3+} complexes embedded in a p(HEMA-co-MMA) polymer organogel (HEMA stands for hydroxyethyl methacrylate and MMA for methyl methacrylate). This system was sensitive to changes to the H^+ and F^- input ions (logical inputs) and the logic outputs are defined analysing the emission intensity at 388 (ascribed to ligand emission), 490 (Tb^{3+} $^5D_4 \rightarrow {}^7F_6$), and 615 nm ($Eu^{3+}$, $^5D_0 \rightarrow {}^7F_2$). The response of these systems defines reverse-IMPLICATION, NOR, and TRANSFER logic gates (Fig. 5). The TRANSFER gate needs to be referred to either one of its two inputs (input 1 or input 2 arbitrarily), for example, TRANSFER (input1) logic gates can be achieved operationally by a YES gate acting on input 1 alone whereas input 2 is not involved with the gate at all. The same group reported Au nanoparticles functionalized with Tb^{3+} and Eu^{3+} complexes performing logic operations in 2017.[65] The response of the emission intensity nanoparticles to the concentration of molecular oxygen (O_2) and of the proton, H^+ was studied as inputs. The ligands used to sensitize the Ln^{3+} were the 4,4,4-trifluoro-1(naphthalene-2-yl)butane(nta)

1,3 dione-4(dimethylamino)benzoic acid (DMAB). Intriguingly, the H^+ ion was used as a double input: Inputs 1 and 2, defined as the sequential increases in the order of magnitude of H^+ concentration by 4 (corresponding to an increase of the pH value of 4 units). The logic outputs were defined monitoring the change in the Eu^{3+} and Tb^{3+} emissions induced by the pH (H^+ concentration). The developed logic functions correspond to NAND and XOR combinatorial logic gates for the emissions originated in the Eu^{3+} and Tb^{3+} ions, respectively. A further step was to combine the NAND and XOR operations to describe a HALF-SUBTRACTOR. Another set of inputs was evaluated for the same system: the excess concentration of the ligands nta, and DMBA. When the concentration of nta or DMAB was equal to 120 times the one of Au nanoparticles, the logic inputs are set to 1. Only in the presence of nta is the Eu^{3+} emission present, and the logic output is set to 1, describing a YES logic gate. The Tb^{3+} emission intensity gives a logical value of 1 in the presence of DMAB (0 when the logic input related to nta is present) corresponding to an INHIBIT logic gate (Fig. 4c). The two-logic inputs system is a TRANSFER logic gate.

There are several reports focused on systems sensitive to the concentration of H^+. In a recent work Z. Zhou et al.[66] reported the Eu (nta)$_3$L@polystyrene and the H^+ and ClO^- ions for logic inputs (L stands for ligand 4′-(4′-vinyl-[1,1′-biphenyl]-4-yl)-2,2′:6′,2″-terpyridine). The intensity ratio between two emission bands (ascribed to the ligand/$^5D_0 \rightarrow {}^7F_2$ transition of Eu^{3+}) was used as the logic output. The intensity ratio decreases nearly linearly with the increase of the ClO^- concentration from 0 to 14 μM. The peak intensity at 400 nm decreases with the increase of the H^+ concentration, and the emission peak is shifted from 420 to 500 nm, remaining then unaltered if the acidity of the medium is further increased. Based on the collaborative response of the H^+ and ClO^- ions, the reported system constitutes a typical two-inputs logic gate for the monitoring presence of the former ion. The logic gate operation was demonstrated using 10 μM ClO^- and 3 equivalent H^+ as inputs, the logical values 0 and 1 referring to the presence or absence of the ClO^- ions. The response of the system resembles an AND and NAND logic gates considering the emission from the ligand or the Eu^{3+}, respectively (Fig. 4d). Remarkably, the output was defined as a ratio between the emission intensities which is independent of the experimental conditions used for detection. The chosen ions make this system interesting in detection applications, despite the short operative range of detection that constitutes a practical limitation.

Another example aiming at the detection of relevant ions and not only the AND gate, but also more complex logic operations, was reported by Y. Yu et al.[71] An upconversion system based on NaYF$_4$:Tm^{3+},Yb^{3+} as the energy transfer donor, and the Rhodamine 6G functionalized PEI (polyethyleneimine) (denoted as RFP), as the energy acceptor, was developed for sensing H^+, OH^-, Cu^{2+}, I^- and S^{2-} ions. The presence of amine groups in the structure of the polyethyleneimine enables the recognition of specific elements and the interaction with these molecules leads to an enhancement or quenching of the luminescence emission, due to energy transfer or electron
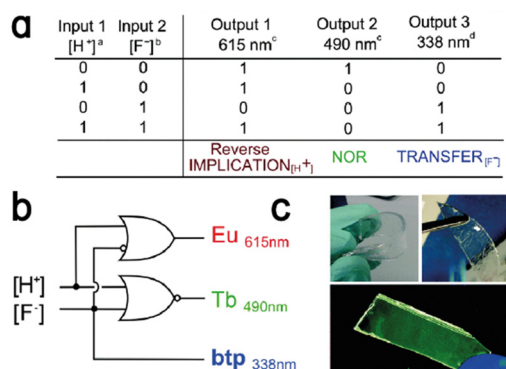

	Input 1 [H⁺]ᵃ	Input 2 [F⁻]ᵇ	Output 1 615 nmᶜ	Output 2 490 nmᶜ	Output 3 338 nmᵈ
	0	0	1	1	0
	1	0	1	0	0
	0	1	0	0	1
	1	1	1	0	1
			Reverse IMPLICATION$_{[H^+]}$	NOR	TRANSFER$_{[F^-]}$

Fig. 5 (a) Truth table of the logic functions. (a) $[H^+]$ = 2 mM; (b) $[F^-]$ = 1 mM. (b) Circuit diagram representation of the logic gate functions. (c) Photographs of Eu^{3+} and Tb^{3+} complexes incorporated gels swollen in H_2O (left) and CH_3OH (right) under ambient light; and after drying and irradiation at 254 nm demonstrating the (0,0) state. Reproduced with permission from ref. 70. Copyright 2015 Royal Society of Chemistry.

transfer processes. The Boolean logic systems are single-input logic gates YES, NOT, dual-input logic gates AND, OR, NOR and INHIBIT, and multiple-input complex logic gates (INHIBIT + OR). The logic output results from the upconversion broadband emission in the 525–635 nm spectral range upon 980 nm excitation. YES and NOT logic gates were defined using, respectively, the H^+ and OH^- concentrations as the logic inputs. To define the AND gate, the broadband is displayed when simultaneously both the RFP and the H^+ are present. Moreover, exploiting $NaYF_4$-RFP-H^+-Cu^{2+}, this system acts as an OR logic gate when the S^{2-} and I^- ions are defining the logic inputs. For $NaYF_4$-RFP-H^+ it is possible to define a NOR logic gate using Cu^{2+} and OH^- as the logic inputs since these two ions lead to a quenching of the emission. The $NaYF_4$-RFP system is an INHIBIT logic gate when the H^+ and Cu^{2+} ions are used as the logic inputs. In a further step, an $NaYF_4$-RFP system was reported, responding to three logic inputs (H^+, Cu^{2+}, OH^-) making the combination between INHIBIT and OR logic gates possible (Fig. 6).

F. Pu et al. in 2014[72] investigated the encapsulation of coordination polymer NPs made from nucleotides and Ln^{3+} ions (Ln = Eu, Tb). The main goal was the formation of coordination polymer nanoparticles with efficient fluorescence enhancement during the self-assembly process of nucleotides, Ln^{3+}, and a dye. The system under study is based on Guanosine 5′-monophosphate (GMP) in combination with Eu^{3+} and Tb^{3+} ions to encapsulate N-methyl mesoporphyrin (NMM), an asymmetrical anionic porphyrin. The NMM exhibited a high emission intensity in the presence of G-quadruplex (nucleic acids that are rich in guanine), DNA, and GMP. Incorporating the NMM with the lanthanides-GMP system, an enhancement of the emission intensity of the transition $^5D_0 \rightarrow {^7F_2}$, at 612 nm, was observed. The first logic gate reported by the authors exploits two logic inputs, the presence (logical value 1) and absence (0) of Eu^{3+} and NMM. Only when both molecules are present (both logic inputs with the Boolean value of 1), was it possible to have a significant increase in the emission intensity at 612 nm (defined as the logical output), defining an AND logic gate (Fig. 7a). The same authors introduced the Tb^{3+} ion together with the Eu^{3+} one and described the resultant logic system based on the presence of the Ln^{3+} ions as the logic inputs. This approach made it possible to recognize the OR logic gate (Fig. 7b), as each or both logic inputs are simultaneously
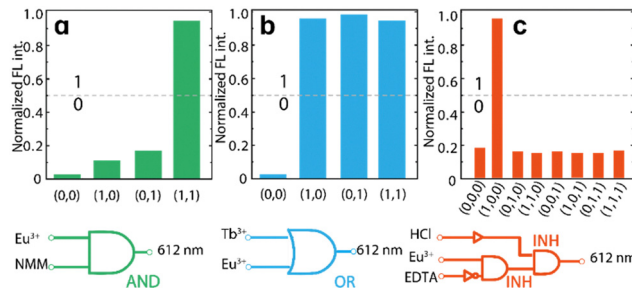

Fig. 6 Logic operations are described by Yu et al. through a system based on $NaYF_4$:Tm^{3+},Yb^{3+}. Adapted with permission from ref. 71. Copyright 2020 Elsevier B.V.

Fig. 7 (a) AND, (b) OR and (c) INH logic operations reported by F. Pu et al. Adapted with permission from ref. 72. Copyright 2013, Wiley-VCH Verlag GmbH & Co. KGaA, Weinheim.

present (logical value 1) the system gives an emission at 612 nm that is signed as the logical value 1. The further step of this work consisted in testing the influence of the chelator ethylenediaminetetraacetic acid (EDTA) on the systems with both Ln^{3+} complexes present. Under this condition, the NMM molecules were released and dispersed into the solution within one minute. The authors observed that the luminescence intensity decreases by introducing EDTA. So, exploiting the Eu^{3+} and EDTA species as the logic inputs the system acts as an INH logic gate. Evaluating the influence of pH on the system and having again EDTA as the first logic input and HCl as the second one, leads to the definition of a NOR logic gate.

Finally, several concatenated logic gates were realized using three inputs: a logic circuit composed of two concatenated INH gates was realized when Eu^{3+}, EDTA, and HCl were logic inputs for the system, being each of the INH gates activated by two logic input signals as depicted in Fig. 7c. A XNOR gate and an AND gate were concatenated using as inputs Eu^{3+}, HCl, and NaOH, and the concatenation of a OR and an INH gate was achieved using Eu^{3+}, Tb^{3+}, and EDTA as inputs. For all the concatenation gates the final output is the Eu^{3+} red emission at 612 nm.

Ln^{3+}-based molecular gates actuated by physical inputs

There is still a lack of reports of molecular logic systems based on Ln^{3+} actuated exclusively by physical inputs. Physical inputs are important because of the input–output homogeneity, no contamination, easy concatenation in complex circuits, and the ability to reuse the device for several cycles.

The first work, from 2004, by Liu et al., reported Ln^{3+} and physical parameters that control the luminescence properties of the emitting centres as the logic inputs. The system was composed of Eu^{3+}-based calixarene systems, using the excitation radiation (logical input 1 was ultraviolet radiation, in the 300–400 nm spectral range) and visible light (logical input 2, in the spectral range over 500 nm). It was possible to switch from a colourless to a coloured isomer (called Calix-2SP and Calix-2MC, respectively). A NOT gate was described using UV radiation as the logic input 1 and the emission intensity at 616 nm (Eu^{3+} $^5D_0 \rightarrow {^7F_2}$ transition) as the logic output.[73] Despite the simplicity of the approach, this is one of the first examples in which ultraviolet radiation and visible light are used as physical inputs.
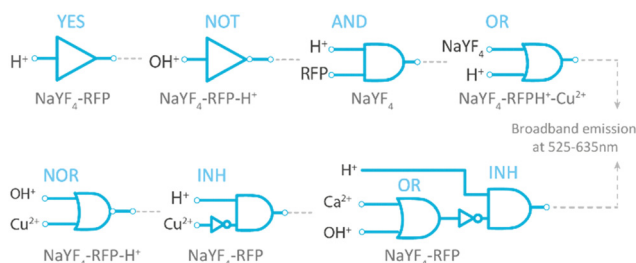
In 2019, H. Fan et al.[74] reported logic device systems based on Eu^{3+}-doped YPO_4 and Pr^{3+}-doped YPO_4 crystals performing INVERTER, NOT, and NAND gates using as inputs the delay time and the power density of two Nd: YAG lasers. The intensity of Eu^{3+} emission at 592 nm ($^5D_0 \rightarrow {}^7F_{0,1}$ transitions) was used to define the logic output. The energy level transition of Eu^{3+}:YPO_4 and Pr^{3+}:YPO_4 with different phases was studied using lasers and the response of the sample depends on the structure and phase symmetry of the YPO_4 host. By modulating different parameters of single and double lasers (power, detuning, and gate delay), it was noticed the energy level transitioned from a single to multi-level with a single laser, and from a single-to-single level with a double laser. The potential of the system is pictured for quantum optics and quantum gates.

In 2020 Nie et al.[75] investigated the upconversion (UC) NPs for molecular logic operations, based on dual excitation wavelength in an Er^{3+} doped β-$NaYF_4$ system. To define the logic gates, two external excitation laser sources (input 1: 1550 nm and input 2: 1064 nm) were used, and the UC emission intensities were exploited to define the logic outputs. Elementary logic operations (OR, AND, and YES) were implemented by studying the change in two emission bands (emission of Er^{3+} in the green and red spectral ranges). The AND logic gate was described using the emission of Er^{3+} in the red spectral range when the power density of the 1064 nm excitation laser was 145 mW mm^{-2} and that for the 1550 nm laser is 24 mW mm^{-2}. A YES gate was constructed using the same set of input parameters and analysing the transitions of Er^{3+} in the green spectral region as the logic outputs. Finally, an OR gate was defined, increasing the laser power density of input 1 to 40 mW mm^{-2} and considering the emission intensity of the Er^{3+} ion in the green spectral region to define the logic output.

In some devices it is possible to perform programming of the output, especially using physical inputs. In this regard, Wu et al.[76] reported electrochemical cells based on $NaGdF_4$: Yb/Tm@$NaYF_4$:Eu NPs and PV, standing for 1,1′-bis(2-phosphonoethyl)-4,4′-bipyridinium dichloride, defined as Eu-UCNPS/ PV, that responds to the excitation by the NIR laser (980 nm) and the alternating electric field. The inputs were defined by the presence of the laser excitation (1 when the laser is active and 0 for the complementary condition) and by the sign of the alternate current (positive or negative). The Eu-UCNPS/PV platform shows emission peaks at 454 and 615 nm after the laser excitation and reversible resonance between Eu-UCNPS and PV with the alternate current. The basic AND gates are defined by taking the red ($^5D_0 \rightarrow {}^7F_2$) emission of Eu^{3+} as the output. The further step was to encode information (in the case of the roman letters "NUS") with a specific sequence where the voltage is responsible for writing and erasing (Fig. 8).

The electrical signal encrypting the information is transmitted to the UCNP/PV where it is transformed into upconverted emitted photons. Some works were published by our research group. In 2016 our group used the emission intensity ratio originating in Eu^{3+} and Tb^{3+} centres as logic outputs, and the excitation radiation and the temperature as logic inputs for reporting AND, INIBITH, and DEMUX logic gates.[77]
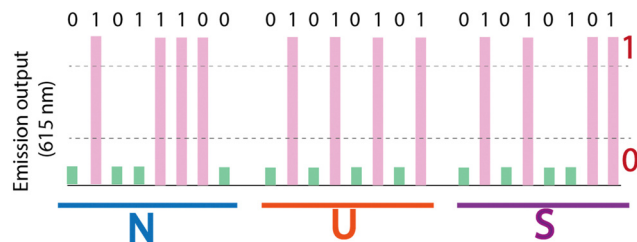

Fig. 8 NUS roman letters encoded information. Adapted with permission from ref. 76. Copyright 2021, Springer Nature, The Author(s), licensed under a Creative Commons Attribution (CC by 3.0) License.

A further study focused on more complex operations was developed in a more recent work published in 2020.[78] The second system reported by us was based on Si-functionalized surfaces with self-assembled monolayers incorporating the Ln^{3+}. By exploiting the Eu^{3+} and Tb^{3+} emission, the platforms render basic (AND, INH, XOR, DEMUX), sequential (KEYPAD LOCK), and arithmetic (HALF ADDER and HALF SUBTRACTOR) logic operations. Moreover, an INHIBIT and an AND logic gate, as well as their combination, were used to design a 1:2 demultiplexer (DEMUX) logic gate, using the UV excitation at 271 nm as one logic input (UV, 0 and 1 logical values – light OFF/ON respectively) and the temperature increase as the second logic input (ΔT, the logical value of 0 when the temperature controller is switched off, 1 instead when is on). To describe the INH1 gate, the intensity ratio $^5D_4 \rightarrow {}^7F_5/{}^5D_0 \rightarrow {}^7F_2$ (of Tb^{3+} and Eu^{3+} transitions, respectively) was set as the logic output (I_1/I_2). For defining an AND gate, the intensity peak ratio (I_{3A}/I_{3B}, two Stark components of the Eu^{3+} $^5D_0 \rightarrow {}^7F_4$ transition) was chosen (Fig. 9). For the XOR gate, the output chosen was the thermal relative sensitivity defined as the first derivative of the intensity ratio (I_1/I_2) with the temperature. Combining AND with XOR gate, and INH with XOR gate HALF-ADDER and HALF-SUBSTRACTOR were defined, respectively. In the end, a KEYPAD LOCK was also implemented using the temperature increment ΔT (0 the heating is off and when is on is 1) and a characteristic temperature T_c (313 K, defined by the intercept temperature of the two linear regimes) as the logic inputs. Only respecting the correct sequence of the
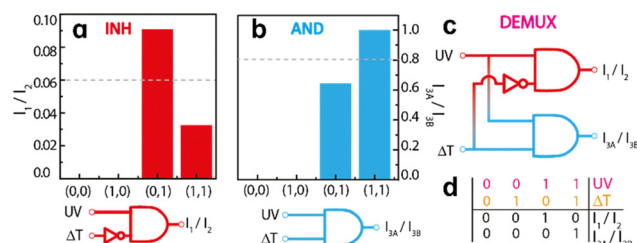

Fig. 9 (a and b) Bar plot and logic operations of the I_1/I_2 and I_{3A}/I_{3B} intensity ratios of the system displaying a transfer function of inhibiting 1 (INH1) and AND logic gates, respectively. (c) Combining the INH1 and AND logic gates, the demultiplexer gate (DEMUX) is obtained. (d) The truth table for the DEMUX gate. Figure adapted with permission. Adapted with permission from ref. 78. Copyright 2022, Wiley-VCH Verlag GmbH & Co. KGaA, Weinheim.

logic inputs, *i.e.*, first ΔT and imposing the system at T_c was it possible to have the logic output 1.

Recently we reported on reconfigurable and reprogrammable logic gates.[79] The system studied is an organic–inorganic hybrid (denoted by di-ureasil) doped with a bi-nuclear Eu^{3+}/Tb^{3+} complex. First, we defined logic operations exploiting two different wavelengths in the UV range (254 and 365 nm) as the logic inputs and as outputs the luminescence intensity quantified in terms of radiance measurements.

Analysing the emissions ascribed to the hybrid host (green-blue spectral region), the $^5D_4 \rightarrow {}^7F_5$ and $^5D_0 \rightarrow {}^7F_2$ transitions of Tb^{3+} and Eu^{3+} respectively, the system performs one INH and two AND gates (Fig. 10a–c). With this first approach, we can demonstrate that the system is reconfigurable since it is possible to define different logic operations by changing the readout selected. The next step was to use the experimental parameters of the time-resolved emission, such as integration time (W) and starting delay (D), to discriminate the different temporal dynamics of the distinct emitting centres present in the system. It was already reported in the literature that the lifetimes of the hybrid, Tb^{3+} are temperature dependent, while the lifetimes of Eu^{3+} are temperature independent, we exploit these differences to define reconfigurable and reprogrammable gates. On one hand, using D and the temperature (T) as inputs is possible to define a reconfigurable gate that can change from INH to NAND gate depending on the selected output. I_1/I_3 output relates the hybrid and Eu emissions, and it is positive only at low temperature and longer D due to the intrinsic lifetime of the material leading to the definition of an INH gate. I_2/I_3 output relates the Tb and Eu emissions, and it is negative only for short D and 298 K (NAND). On the other hand, defining W and D as inputs it is possible to produce temperature driven changes in the luminescence of the material, in this case it is possible to tune the I_2/I_3 output in two different ranges of temperatures; in this way the system is described as temperature reprogrammable from INH to AND (Fig. 10d–f).

The described logic device is required to work at two different temperatures (14 and 298 K), which is not a final engineering solution in terms of applications in real-world electronic devices. A more feasible range of temperature as the physical input was chosen in our latest work.[80]

Exploiting the temperature driven changes in the luminescence of a similar Tb^{3+}–Eu^{3+} co-doped hybrid material, along with the influence of the abovementioned D and W detection parameters, we recently reported an all-photonic temperature-reprogrammable optical filter.[80] For this purpose, the temperature changes on the luminescence of the material were rationalized in terms of a transfer function H parameter that relates ratiometric parameters involving the integrated intensity ratio between the main transitions of Tb^{3+} and Eu^{3+} as a function of the detection frequency (f), defined as W^{-1}. This parameter displays an opposite temperature driven behaviour when the temperature is below and above a turning point temperature (T_c), that can be interpreted in terms of the classical bode plot of conventional resistor–capacitor (RC) electrical circuit passive pass filters, *i.e.*, low-pass filter and high pass filter for temperatures below and above T_c respectively. This illustrative system presents remarkable features and advantages over conventional filters. The nature and order of the hybrid material as a filter can be freely modified with the temperature and D respectively while the optical signal of the material can be chosen with f, all of this, using the same material without any addition of extra elements to the system. In contrast, changes in the nature (high pass or low pass) and order (filtering power) of conventional electronic RC circuit passive filters imply important modifications in their circuitry configuration precluding any reconvertibility using the same circuit. This work shows a firm step toward the design and development of molecular analogs of conventional circuit electrical passive components.[80]

Very recently we demonstrated the application of BiF_3:YbEr sub-micro particles for defining molecular logic operations.[81] We described a molecular chipset of four logic gates (AND, NAND, NOR and NOT) setting as inputs the temperature (logic value 0 for 305 K, and 1 for 360 K) and the power density (logic value of 0 at 5 W cm^{-2}, and 1 at 111 W cm^{-2}). For digitalizing the output, we calculated the intensity of some Stark components of Er^{3+} transitions $^4S_{3/2} \rightarrow {}^4I_{15/2}$, and $^2H_{11/2} \rightarrow {}^4I_{15/2}$ (labelled from I_1 to I_6), then we defined four ratiometric outputs (R_{1-4}) that allowed us to describe the four logic operations (Fig. 11). In summary, our research group provides a physical perspective on the development of molecular logic. This is achieved by leveraging our expertise in the development of luminescent molecular sensors and other luminescent devices, to explore innovative approaches to molecular logic. The field of photoluminescent molecular logic gates focuses on two primary areas of research: the first is the development of molecular logic gates that can function as electronic devices
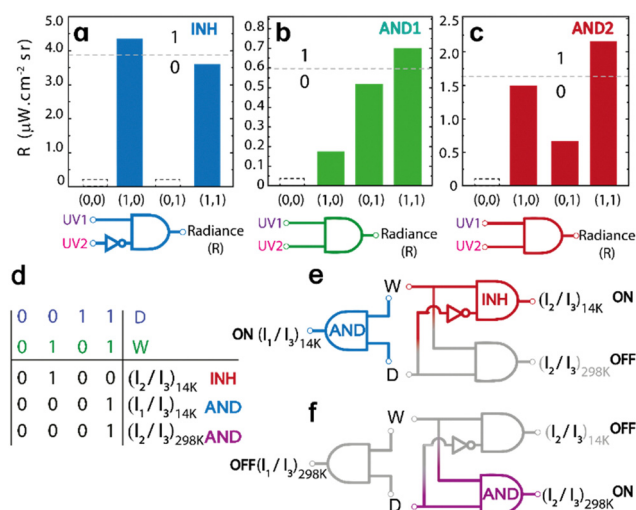

Fig. 10 (a–c) Bar plots diagrams describing different logic operations defined through the hybrid, Tb^{3+}, and Eu^{3+} emissions. UV1 and UV2 are the inputs associated with the 365 nm and 254 nm UV lamps. (d) True table of the reprogrammable gates (e and f) INH and AND gates described through the I_1/I_3 and I_2/I_3 output at 298 K and 14 K. Adapted with permission from ref. 79. Copyright 2022, Wiley-VCH Verlag GmbH & Co. KGaA, Weinheim.
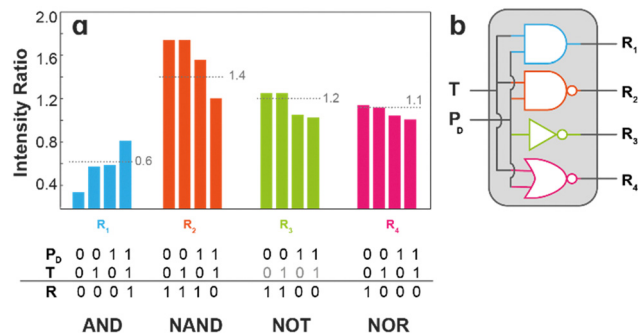
Fig. 11 (a) Bar chart of the intensity ratios $R1$–$R4$ as a function of the temperature input (T) and excitation power density (P_D) presenting the corresponding threshold (pointed line) the truth tables in the bottom. (b) Schematic representation of the logic circuitry with the logic gates presented in (a). Figure reproduced from ref. 81.

using exclusively physical inputs; whereas the second consists on the design of advanced molecular logic circuits based on the intrinsic photophysical properties of luminescent centres such as the Ln^{3+} ions. By better understanding the physical principles governing the photoluminescent properties of these emitting centres, one may design create photonic equivalents to small electronic devices using a single ion as the computing element.

Conclusion

Molecular logic is a research field studying molecules for performing logic functions. The field is evolving towards sensing namely for biological relevant ions with interest detection.[32,82] In this case, the reproducibility and working in wet conditions are not necessary for the purpose of molecular logic functions defined. Nowadays the amazing development of synthetic methods has put the field in such a point that it is possible to rationally design numerous materials, namely those involving light-emitting centres, such as the Ln^{3+} ions.

The logic systems based on Ln^{3+} ions developed so far are essentially chemical sensors able to detect a small amount of a chemical specie in large populations, which is particularly relevant to biotechnological applications namely inside living cells. However, it is established that the Ln^{3+} ions respond also to physical stimuli such as temperature, pressure, photons with distinct wavelengths, from X-rays to NIR, or electric or magnetic field, despite the very few reports on logic applications of these inputs. As is well known, Ln^{3+} ions present narrow emitting lines and several emission features (*e.g.* intensity of emission, lifetimes, *etc.*) that can virtually perform several multiplexing and parallel processing.

We foresee that the development of molecular logic functions based on Ln^{3+}-ions can leverage molecular logic by exploiting hybrid systems that are able to communicate with the established electronic devices and perform computing based on molecular logic gates, delivering the computation output with gains in the information processing throughput. Besides that, these ions can mimic diverse logic gates and the

technology previously developed in the context of optical communications can be effortlessly adapted to develop hybrid photonic–electronic molecular systems, with an electrical interface and a molecular computing unit accessible *via* the photoluminescent properties. Indeed, the Ln^{3+} ions are already widely used in optoelectronics,[83] making it easy to foresee the integration of photonic molecular logic chips with Si-based conventional electric systems, thus acting on the excitation through commercial LED sources and detecting the outputs as electrical signals *via* photodetectors, in what could be hypothesized as a hybrid photonic–electronic system.

Moreover, many physical inputs have the potential to be exploited with several advantages eventually yielding concatenation, or integration in solid state components. This may enable the on-demand design of molecular combinatorial logic gates, keylock devices, and memories with remote access using external stimuli (the radiation, heat, electric or magnetic field, *etc.*) or even other parameters that modify the photophysical properties of the Ln^{3+} ions (excitation in continuous or pulsed mode, time-resolved detection, *etc.*) as the logic inputs.

We believe that in the years to come the reports on molecular logic systems will be essentially on basic research stressing that the field is still not mature enough for replacing components of conventional computers, and thus a full molecular computer is yet not forecasted. However, we consider that there are innovative and disruptive approaches to molecular computing that should be exploited to evaluate their potential as molecular equivalents to electronic devices, in particular those involving the intriguing photophysical properties of Ln^{3+} ions. These ions show promising directions for creating molecular logic functions using photoluminescence that could operate either in biological systems or be integrated with current electronic computing systems.

As the current electronics circuits are benefiting from long term research and most probably the future implementations of molecular logics may be grounded on a hybrid system that combines well implemented electronic circuits with molecular counterparts. While the former can deliver cost-effective devices, the later can potentially deliver high-density information processing, low power consumption, and compatibility with a diversity of inputs, both of chemical and physical nature. Electronic circuits provide the infrastructure for signal amplification, transmission, and control, while molecular logic brings new functionalities and the ability to interface with chemical and biological systems. Various methods have been explored for connecting molecular logic gates to electronic components, such as using molecular wires,[84] nanoscale electrodes,[85] or self-assembled monolayers.[86] Such molecular-scale devices offer the potential for ultra-compact and energy-efficient computing systems, although it presents both opportunities and challenges: on one hand, it opens intriguing possibilities for designing advanced computing systems with enhanced functionalities; but on the other hand, it requires addressing technical hurdles such as device compatibility, signal propagation, and scalability.

In summary, insights into the direction of this field suggest that it holds great promise for the development of new types of

computing systems that are more efficient, versatile, and adaptable than conventional silicon-based technologies. Moreover, molecular logic-based computation has the potential to revolutionize many fields, from medicine to environmental monitoring, by enabling the development of low-cost, portable, and highly sensitive diagnostic and sensing tools. However, there are still many challenges to overcome, such as:

Scalability

One of the main challenges facing molecular logic is scaling up the technology to produce functional devices and systems that can perform complex computations. Currently, most molecular logic devices are only capable of performing simple logic operations and are not yet scalable to the level required for practical applications. Taking advantage of the widespread use of Ln^{3+}-based materials in the fibre-optics industry, some gates can be opened if molecular logics can be implemented using these intriguing luminescent probes.

Robustness and reliability

Molecular logic devices are often sensitive to changes in their environment, such as temperature, pH, and the presence of contaminants. Ensuring the robustness and reliability of molecular logic devices is critical for their successful integration into practical applications. The main advantage of the logic computing using Ln^{3+} ions in the solid state is their virtual independence of many of these parameters, which make them very attractable for molecular logics.

Integration with conventional electronic circuits

To be useful in practical applications, molecular logic devices need to be integrated with conventional electronic circuits, which can be challenging due to the differences in operating principles and materials. In this the point of the technology, the Ln^{3+} ions are prevalent in many photonic devices and thus the integration with current electronic devices is possible using hybrid electronic–photonic devices.

Design and synthesis of novel molecules for logic

Designing and synthesizing complex molecules that can perform specific logic functions is still a significant challenge. Developing a library of such molecules could greatly accelerate progress in the field of molecular logics. Taking advantage of the well-known properties of the Ln^{3+}-ions will probably open the possibility of producing relevant computational outcomes using the physics ruling out the photophysical properties of these ions.

Cost-effectiveness

Currently, the cost of synthesizing and characterizing molecular logic devices is relatively high, as these are only proof-of-concept devices. Developing cost-effective methods for producing and characterizing these devices will be essential for their widespread adoption and commercialization. In this point there is a clear advantage in the production and commercialization of Ln^{3+}-based materials because the technology to produce these materials was maturated with the emergence of the optical communications.

Nonetheless, the field is rapidly evolving, and new discoveries and breakthroughs are expected to lead to exciting applications and opportunities soon, such as the perspective of developing a lanthanide-based logic, a venture that can benefit the future of molecular computing.

Author contributions

SZ: writing – original draft and figures adaptation and preparation. MAH-R, RASF, CDSB: conceptualization, supervision, writing – reviewing and editing.

Conflicts of interest

There are no conflicts to declare.

Acknowledgements

References

1 B. Randell, *The Origins of Digital Computer*, Springer, 1982, pp. 349–354.
2 A. P. de Silva and S. Uchiyama, *Nat. Nanotechnol.*, 2007, **2**, 399–410.
3 T. Baehr-Jones, T. Pinguet, P. Lo Guo-Qiang, S. Danziger, D. Prather and M. Hochberg, *Nat. Photonics*, 2012, **6**, 206–208.
4 B. Daly, T. S. Moody, A. J. M. Huxley, C. Yao, B. Schazmann, A. Alves-Areias, J. F. Malone, H. Q. N. Gunaratne, P. Nockemann and A. P. de Silva, *Nat. Commun.*, 2019, **10**, 49.
5 P. Ball, *Nature*, 2000, **406**, 118–120.
6 T. D. Ladd, F. Jelezko, R. Laflamme, Y. Nakamura, C. Monroe and J. L. O'Brien, *Nature*, 2010, **464**, 45–53.
7 M. Conrad, in *Advances in Computers*, ed. M. C. Yovits, Elsevier, 1990, vol. 31, pp. 235–324.
8 J.-Y. Mao, L. Zhou, X. Zhu, Y. Zhou and S.-T. Han, *Adv. Opt. Mater.*, 2019, **7**, 1900766.
9 A. P. de Silva, N. H. Q. Gunaratne and C. P. McCoy, *Nature*, 1993, **364**, 42–44.
10 A. P. de Silva and N. D. McClenaghan, *J. Am. Chem. Soc.*, 2000, **122**, 3965–3966.
11 J. Ling, B. Daly, V. A. D. Silverson and A. P. de Silva, *Chem. Commun.*, 2015, **51**, 8403–8409.
12 S. Erbas-Cakmak, S. Kolemen, A. C. Sedgwick, T. Gunnlaugsson, T. D. James, J. Yoon and E. U. Akkaya, *Chem. Soc. Rev.*, 2018, **47**, 2228–2248.
13 D. Margulies, C. E. Felder, G. Melman and A. Shanzer, *J. Am. Chem. Soc.*, 2007, **129**, 347–354.

14 F. Nicoli, E. Paltrinieri, M. Tranfić Bakić, M. Baroncini, S. Silvi and A. Credi, *Coord. Chem. Rev.*, 2021, **428**, 213589.
15 Y. Hirshberg, *J. Am. Chem. Soc.*, 1956, **78**(10), 2304.
16 A. Aviram and M. A. Ratner, *Chem. Phys. Lett.*, 1974, **29**, 277–283.
17 D. Parker, *Chem. Commun.*, 1998, 245–246.
18 T. Gunnlaugsson, D. A. Mac Dónail and D. Parker, *Chem. Commun.*, 2000, 93–94.
19 S. Sahu, T. B. Sil, M. Das and G. G. Krishnamoorthy, *Analyst*, 2015, **140**, 6114–6123.
20 M. Karar, P. Paul, B. Biswas, A. Mallick and T. Majumdar, *J. Chem. Phys.*, 2020, **152**, 075102.
21 D. Nilsson, N. Robinson, M. Berggren and R. Forchheimer, *Adv. Mater.*, 2005, **17**, 353–358.
22 A. J. Genot, J. Bath and A. J. Turberfield, *J. Am. Chem. Soc.*, 2011, **133**, 20080–20083.
23 D. Halder, A. Mallick and P. Purkayastha, *Langmuir*, 2019, **35**, 10885–10889.
24 J. Andréasson, U. Pischel, S. D. Straight, T. A. Moore, A. L. Moore and D. Gust, *J. Am. Chem. Soc.*, 2011, **133**, 11641–11648.
25 Q. Hao, Z.-J. Li, B. Bai, X. Zhang, Y.-W. Zhong, L.-J. Wan and D. Wang, *Angew. Chem., Int. Ed.*, 2021, **60**, 12498–12503.
26 E. Katz, *Molecular and supramolecular information processing: from molecular switches to logic systems*, John Wiley & Sons, New York, 2013.
27 H. Komatsu, S. Matsumoto, S. Tamaru, K. Kaneko, M. Ikeda and I. Hamachi, *J. Am. Chem. Soc.*, 2009, **131**, 5580–5585.
28 P. L. Gentili, *J. Phys. Chem. A*, 2008, **112**, 11992–11997.
29 F. Pu, J. Ren, X. Yang and X. Qu, *Chem. – Eur. J.*, 2011, **17**, 9590–9594.
30 W. T. Huang, H. Q. Luo and N. B. Li., *Anal. Chem.*, 2014, **86**, 4494–4500.
31 F. Pu, C. Wang, D. Hu, Z. Huang, J. Ren, S. Wang and X. Qu, *Mol. BioSyst.*, 2010, **6**, 1928–1932.
32 E. Katz, *Enzyme-Based Computing Systems*, John Wiley & Sons, New York, 2019.
33 C. Zhang, J. Yang and J. Xu, *Chin. Sci. Bull.*, 2011, **56**, 3566–3571.
34 P. T. Mathew and F. Fang, *Engineering*, 2018, **4**, 760–771.
35 S. Erbas-Cakmak and E. U. Akkaya, *Angew. Chem., Int. Ed.*, 2013, **52**, 11364–11368.
36 T. Niazov, R. Baron, E. Katz, O. Lioubashevski and I. Willner, *Proc. Natl. Acad. Sci. U. S. A.*, 2006, **103**, 17160–17163.
37 M. Elstner, J. Axthelm and A. Schiller, *Angew. Chem., Int. Ed.*, 2014, **53**, 733.
38 C. Yao, J. Ling, L. Chen and A. P. de Silva, *Chem. Sci.*, 2019, **10**, 2272–2279.
39 J. Hatay, L. Motiei and D. Margulies, *J. Am. Chem. Soc.*, 2017, **139**, 2136.
40 D. S. M. N. Stojanovic and S. Rudchenko, *Acc. Chem. Res.*, 2014, **47**, 1845.
41 K. Pilarczyk, E. Wlaźlak, D. Przyczyna, A. Blachecki, A. Podborska, V. Anathasiou, Z. Konkoli and K. Szaciłowski, *Coord. Chem. Rev.*, 2018, **365**, 23–40.
42 L. Liu, P. Liu, L. Ga and J. Ai, *ACS Omega*, 2021, **6**, 30189–30204.
43 C.-Y. Yao, H.-Y. Lin, H. S. N. Crory and A. P. de Silva, *Mol. Syst. Des. Eng.*, 2020, **5**, 1325–1353.
44 D. C. Magri, *Coord. Chem. Rev.*, 2021, **426**, 213598.
45 A. P. de Silva, *Molecular-Logic based Computation*, Royal Society of Chemistry, Cambridge, UK, 2013.
46 K. Szacilowski, *Infochemistry: information processing at the nanoscale*, John Wiley & Sons, United Kingdom, 2012.
47 L. Gu, C. P. Zhang, A. F. Niu, J. Li, G. Y. Zhang, Y. M. Wang, M. R. Tong, J. L. Pan, Q. W. Song, B. Parsons and R. R. Birge, *Opt. Commun.*, 1996, **131**, 25–30.
48 H. Tian, B. Qin, R. Yao, X. Zhao and S. Yang, *Adv. Mater.*, 2003, **15**, 2104–2107.
49 X. Guo, D. Zhang, T. Wang and D. Zhu, *Chem. Commun.*, 2003, 914–915.
50 X. Chai, Y.-X. Fu, T. D. James, J. Zhang, X.-P. He and H. Tian, *Chem. Commun.*, 2017, **53**, 9494–9497.
51 J. Andréasson and U. Pischel, *Chem. Soc. Rev.*, 2010, **39**, 174–188.
52 J. Andréasson and U. Pischel, *Coord. Chem. Rev.*, 2021, **429**, 213695.
53 J.-C. G. Bünzli, N. André, M. Elhabiri, G. Muller and C. Piguet, *J. Alloys Compd.*, 2000, **303–304**, 66–74.
54 L. R. Melby, N. J. Rose, E. Abramson and J. C. Caris, *J. Am. Chem. Soc.*, 1964, **86**, 5117–5125.
55 T. Gunnlaugsson and J. Leonard, *Chem. Commun.*, 2005, 3114–3131.
56 X. Y. Xu and B. Yan, *Adv. Funct. Mater.*, 2017, **27**, 1–11.
57 B. Li, D. Zhao, F. Wang, X. Zhang, W. Li and L. Fan, *Dalton Trans.*, 2021, **50**, 14967–14977.
58 J. Yan, B. Li, P. Yang, J. Lin and Y. Dai, *Adv. Funct. Mater.*, 2021, **31**, 2104325.
59 J.-C. G. Bünzli, *Chem. Rev.*, 2010, **110**, 2729–2755.
60 C. Luo, L. He, F. Chen, T. Fu, P. Zhang, Z. Xiao, Y. Liu and W. Tan, *Cell Rep. Phys. Sci.*, 2021, **2**, 100350.
61 D. Tzeli and I. D. Petsalakis, *J. Chem.*, 2019, 1–9.
62 T. Gunnlaugsson, D. A. Mac Dónaill and D. Parker, *J. Am. Chem. Soc.*, 2001, **123**, 12866–12876.
63 L. Wang, B. Li, L. Zhang, P. Li and H. Jiang, *Dyes Pigm.*, 2013, **97**, 26–31.
64 C. S. Bonnet and T. Gunnlaugsson, *New J. Chem.*, 2009, **33**, 1025–1030.
65 L. K. Truman, S. J. Bradberry, S. Comby, O. Kotova and T. Gunnlaugsson, *ChemPhysChem*, 2017, **18**, 1746–1751.
66 Z. Zhou, H. Wu, F. Li, L. Ma and X. Qiao, *Dyes Pigm.*, 2020, **174**, 108033.
67 M. de Sousa, M. Kluciar, S. Abad, M. A. Miranda, B. de Castro and U. Pischel, *Photochem. Photobiol. Sci.*, 2004, **3**, 639–642.
68 H. Chen, J. Cao, P. Zhou, X. Li, Y. Xie, W. Liu and Y. Tang, *Biosens. Bioelectron.*, 2018, **122**, 1–7.
69 L. Lu, C. Chen, D. Zhao, J. Sun and X. Yang, *Anal. Chem.*, 2016, **88**, 1238–1245.
70 S. J. Bradberry, J. P. Byrne, C. P. McCoy and T. Gunnlaugsson, *Chem. Commun.*, 2015, **51**, 16565–16568.
71 Y. Yu, S. Xu, S. Gao, M. Jiang, J. Zhang, X. Li, X. Zhang and B. Chen, *Spectrochim. Acta, Part A*, 2020, **230**, 118047.
72 F. Pu, E. Ju, J. Ren and X. Qu, *Adv. Mater.*, 2014, **26**, 1111–1117.
73 Z. Liu, L. Jiang, Z. Liang and Y. Gao, *Tetrahedron Lett.*, 2005, **46**, 885–887.
74 H. Fan, A. Imran, F. Raza, I. ahmed, K. Amjad, P. Li and Y. Zhang, *RSC Adv.*, 2019, **9**, 38828–38833.
75 J. Nie, W. Ying, J. Gu, F. Wang, S. Xu and S. Liu, *J. Phys. D: Appl. Phys.*, 2020, **53**, 285103.
76 Y. Wu, J. Xu, X. Qin, J. Xu and X. Liu, *Nat. Commun.*, 2021, **12**, 1–7.
77 M. Rodrigues, R. Piñol, G. Antorrena, C. D. S. Brites, N. J. O. Silva, J. L. Murillo, R. Cases, I. Díez, F. Palacio, N. Torras, J. A. Plaza, L. Pérez-García, L. D. Carlos and A. Millán, *Adv. Funct. Mater.*, 2016, **26**, 200–209.
78 M. A. Hernández-Rodríguez, C. D. S. Brites, G. Antorrena, R. Piñol, R. Cases, L. Pérez-García, M. Rodrigues, J. A. Plaza, N. Torras, I. Díez, A. Millán and L. D. Carlos, *Adv. Opt. Mater.*, 2020, **8**, 2000312.
79 S. Zanella, M. A. Hernández-Rodríguez, L. Fu, L. D. Carlos, R. A. S. Ferreira and C. D. S. Brites, *Adv. Opt. Mater.*, 2022, **10**, 2200138.
80 M. A. Hernández-Rodríguez, S. Zanella, L. Fu, A. N. C. Neto, L. D. Carlos and C. D. S. Brites, *Laser Photonics Rev.*, 2023, **17**, 2200877.
81 S. Zanella, E. Trave, E. Moretti, A. Talon, M. Back, L. D. Carlos, R. A. S. Ferreira and C. D. S. Brites, *Front. Photonics*, 2022, **3**, DOI: **10.3389/fphot.2022.1010958**.
82 E. A. Barnoy, R. Popovtzer and D. Fixler, *J. Biophotonics*, 2020, **13**, e202000158.
83 Z. Ahmed and K. Iftikhar, *RSC Adv.*, 2014, **4**, 63696–63711.
84 M. D. Ward, *J. Chem. Educ.*, 2001, **78**, 321–328.
85 S. Roy and Z. Q. Gao, *Nanotechnology*, 2010, **21**, 245306.
86 S. Kim, P. D. Carpenter, R. K. Jean, H. T. Chen, C. W. Zhou, S. Ju and D. B. Janes, *ACS Nano*, 2012, **6**, 7352–7361.